2nd International Conference on Iron-Sulfide Reactions in Concrete
Hilton Mystic | Connecticut | USA | May 13th & May 14th, 2026

# From CT to MA: Case Studies of Crumbled Foundations from Pyrrhotite Oxidation and Internal Sulfate Attack in the Eastern US

**Dipayan Jana** (1)

(1) *Construction Materials Consultants, Inc. and Applied Petrographic Services, Inc.*

## Abstract

Oxidation of pyrrhotite and the resultant internal sulfate attack (ISA) have caused widespread cracking and crumbling of thousands of residential concrete foundations across northeastern CT and central to western MA. Pyrrhotite occurred in the schist and gneiss of the Brimfield Schist formation in the Bronson Hill Anticlinorium formed during a Devonian age mountain-building event (Acadian Orogeny, approximately 416-360 million years ago) from the collision of the ancestral North American continent (Laurentia) with a microcontinent (Avalonia), resulting in the formation of the Appalachian Mountains and large-scale pyrrhotite crystallization along this mountain belt. Case studies are provided from a house of crumbled and replaced foundation in Vernon, CT and two houses in Rutland, MA built in 2002. Typical host rocks of pyrrhotite in the distressed foundations of CT are the dominant garnetiferous quartzo-feldspathic and micaceous schist and gneiss and minor micaceous quartzite supplied from the Becker's Quarry in Willington, CT. Aggregates in the examined foundations from Rutland, MA are mica schist and quartzite from a local quarry that are lithologically distinct from CT but still dominantly schistose rocks. In both cases, close association of pyrrhotite with biotite and the gneissose and schistose textures of rocks have provided pathways for access of moisture and oxygen for oxidation. Pyrrhotite-bearing crushed stone particles in both CT and MA samples are ranged from 50 to 70% of coarse aggregate. Pyrrhotite occurred as: (a) coarse subhedral to anhedral grains in the host schist/gneiss often engulfing minerals from the host rocks, indicating late intrusion from crystallization in hydrothermal vein into preexisting rocks, (b) aligned along the weak planes developed from parallel arrangements of minerals in the schist and gneiss from remobilization during the orogeny, (c) in mica-rich layers of quartzite, and (d) as finely disseminated forms, most of which are mostly present in unoxidized forms in a small fraction of nonreactive aggregates. Oxidized pyrrhotite grains showed characteristic striations from the typical banded microstructure of expansive iron oxyhydroxide strips in the iron sulfide matrix. Pyrrhotite is the dominant iron sulfide in all these rocks (ranging commonly from <10% to occasionally 20 to 50% in the individual aggregates) with minor pyrite, chalcopyrite and trace pentlandite that can be effectively distinguished from their color tones (bronze to brownish-bronze pyrrhotite to pale brass-yellow pyrite to brassy yellow often iridescent chalcopyrite to pale bronze to golden-yellow pentlandite) on the polished sections in reflected-light in a stereomicroscope or a petrographic microscope. Total sulfur contents of concretes ranged from 0.27% in the CT to 0.3-0.5% in MA samples. Extensive cracking is seen during microscopical examinations of fluorescent epoxy-impregnated polished solid and thin sections. SEM-EDS studies were performed on numerous oxidized pyrrhotite grains as well as from ettringite-infested microcracked paste fractions of concrete. XRD studies were done on some individual oxidized pyrrhotite grains to detect the reactive (magnetic, 4C) type of pyrrhotite and oxidation products. Finally, mechanisms of distress from two-stage expansions from pyrrhotite oxidation followed by ISA are discussed.

***Keywords***: *cracking, ISA, oxidation, pyrrhotite, sulfate.*

## 1. INTRODUCTION

Oxidation of pyrrhotite ($Fe_{1-x}S$, $0 < x < 0.125$) in concrete aggregates and the resultant internal sulfate attack (ISA) in paste have caused extensive cracking in thousands of residential concrete foundations across eastern Connecticut and Massachusetts. Case studies on detailed microstructural, chemical, and mineralogical evidence of pyrrhotite oxidation and the resultant internal sulfate attack from many

cracked concrete foundations in CT were previously presented by Jana [1, 2, 3, 4]. At the time of this report, foundations of up to 35,000 homes built between 1983 and 2016 from 56 towns in north, east and central CT, and 10,000 homes from 51 cities and towns in 6 counties in MA (primarily at central MA and along NH and CT borders) are affected by this epidemic. Concrete for the affected homes in CT were primarily sourced from a quarry in Willington, CT operated during 1980s for 30 years that sits in a weathered hydrothermal vein of metamorphic rocks containing significant pyrrhotite mineralization, whereas multiple quarries are reported for crumbled foundations in MA. The present study is an extension of comparative case studies of three additional distressed foundations, one from Vernon, Tolland County in Connecticut and two others from Rutland, N Worchester County in Massachusetts.

### 1.1 CT and MA Legislations

In order to restrict incorporation of pyrrhotite-bearing aggregates into concrete, both CT and MA legislations [5, 6] have adopted a multi-stage screening protocol based on [4] (a) total sulfur content of aggregate ($S_T$) to be less than 0.1% for acceptance, or (b) further examination by petrography, XRD, SEM-EDS, WDXRF for positive detection of pyrrhotite for aggregates having $0.1 \leq S_T < 1.0$, and (c) long-term expansion tests of mortar bars or concrete prisms for aggregates where pyrrhotite is positively identified by petrography, or sale for a period of 1 year until further evaluation if pyrrhotite is not detected.

### 1.2 Mechanism of Two-Stage Expansions

In CT and MA, distress of concrete foundations are (a) primarily due to in situ expansions of unsound aggregates from oxidation of pyrrhotite in the presence of moisture and oxygen to various iron oxides/hydroxides/oxyhydroxides (ferrihydrite, goethite) causing first-stage cracking in concrete from tensile stresses, which is often followed by (b) additional expansions in paste due to attack of the released sulfate/sulfuric acid byproducts of oxidation to various cement hydrates and formation of ettringite (e.g., in CT, MA), or additional thaumasite (e.g., in Canada where pyrrhotite grains are surrounded by an iron carbonate rim, or in a concrete containing crushed limestone as a source of carbonates) in confined spaces to cause additional cracking. Compared to its close cousin, pyrite, even at a level of less than 0.5% by mass of aggregate, pyrrhotite can cause extensive cracking and crumbling of concrete.

### 1.3 Field Evidence of Distress

Extensive cracking of concrete foundation, popouts of exposed fractured oxidized pyrrhotite grains on the surfaces of foundation walls, and white sulfate efflorescence deposits are seen in the Vernon, CT home, which are shown in Ref 7. Ref 7 also provides a detailed optical and SEM microstructural atlas of pyrrhotite oxidation and resultant distress in these three crumbled foundations along with other laboratory data.

## 2. MATERIALS AND METHODS

Multiple broken concrete fragments were received from all three crumbled foundations, which were photographed, documented, and processed for various laboratory studies. Fragments were first sectioned into multiple parallel slices with a water-cooled diamond saw, followed by creating polished sections for examinations in a stereomicroscope, and subsequent trimming of other slices to 50 × 75 mm size blocks for preparation of polished fluorescent dye-mixed epoxy-impregnated thin sections for examinations in stereomicroscope and petrographic microscope *a la* ASTM C 856, and SEM-EDS *a la* ASTM C 1723. Additional pieces were pulverized to fine powders for total sulfur (ASTM D 4239), XRD and XRF studies.

## 3. RESULTS & DISCUSSION

### 3.1 Total Sulfur

$S_T$ of the Vernon, CT foundation is 0.273%, which would have outright discarded the aggregate as per the CT legislation. $S_T$ of the two foundations from MA are 0.302% and 0.506%, which too, as per the MA legislation, would have subjected those aggregates for further examination by petrography.

## 3.2 Petrographic Examinations

Concrete in the Vernon, CT foundation is dense, well-consolidated, and made using ¾-in. (19-mm) nominal size crushed schist-gneiss-quartzite coarse aggregate, $^3/_8$-in. (9.5 mm) nominal size crushed siliceous sand fine aggregate, both coarse and fine aggregates are well-graded and well-distributed, and portland cement paste having an estimated water-cement ratio (*w/c*) of 0.45. Concrete is air-entrained having an estimated air content of 5.5%. Pyrrhotite is detected in the predominant dark gray garnetiferous quartzo-feldspathic and micaceous schist and gneiss, as well as in the subordinate light brown quartz-feldspar-mica gneiss (having a higher quartz content than the dark gray gneiss) and in the lighter micaceous quartzite in coarse aggregate [7], all of which were reportedly quarried from the Brimfield Schist formation in the Becker's Quarry in Willington, CT.

Concrete in the two crumbled foundations from Rutland, MA are equally dense, well-consolidated, and made using ¾-in. (19-mm) nominal size crushed schist and quartzite coarse aggregate, $^3/_8$-in. (9.5 mm) nominal size crushed siliceous sand fine aggregate, both coarse and fine aggregates are well-graded and well-distributed, and a paste of portland cement and fly ash (added at 15-20% by mass of total cementitious materials) having similar water-cementitious materials ratios (*w/cm*) estimated to be 0.44 to 0.48. Concrete is air-entrained having estimated air contents of 5 to 5.5%. Pyrrhotite is detected in mica schist and quartzite in coarse aggregate [7], which was reportedly derived from a local quarry that are lithologically distinct from the aggregate found in the CT foundation but still dominantly composed of schistose rocks of the Brimfield Schist formation.

Almost 60 to 70% of coarse aggregate in CT and 50 to 60% in MA are pyrrhotite-bearing [7]. In all three foundations, pyrrhotite occurred as [7]: (a) coarse subhedral to anhedral grains in the host schist/gneiss often engulfing minerals from the host rocks for late intrusion from crystallization in hydrothermal vein into preexisting rocks, (b) aligned along the weak planes developed from parallel arrangements of micaceous and quartzo-feldspathic minerals in the schist and gneiss from remobilization during the Acadian orogeny, (c) in mica-rich layers of quartzite, and (d) as finely disseminated forms, most of which are mostly present in unoxidized forms in a small fraction of nonreactive aggregates. Other sulfides detected are pyrite, chalcopyrite, and trace pentlandite, which are distinguished from their color tones, e.g., bronze to brownish-bronze pyrrhotite to pale brass-yellow pyrite to brassy yellow often iridescent chalcopyrite to pale bronze to golden-yellow pentlandite. Pyrrhotite contents varied from <10% to occasional 20-50% in individual aggregate grains.

## 3.3 SEM-EDS Studies

SEM-EDS studies of oxidized pyrrhotite grains and associated paste in all three foundations showed five characteristic features [7]: (a) parallel Fe-O oxidized bands in Fe-S oxidized pyrrhotite matrix, (b) pyrite-like stoichiometry of restructured oxidized pyrrhotite in Fe/S atomic ratios when SEM-EDS analyses are done from the Fe-S matrices in between the Fe-O bands, (c) extensive microcracking in the oxidized pyrrhotite grains, often extending into the aggregate and even to the neighbouring paste, (d) secondary ettringite precipitates in cracks and voids but (e) no elevated sulfate levels (S/Ca atomic ratios are mostly within 0.0 and 0.05) in the SEM-EDS data collected from the interstitial paste fractions.

## 3.4 XRD and XRF

For CT foundation, XRD result of bulk concrete showed [7]: (a) albite 39.4%, quartz 18.5%, microcline 4.1%, orthoclase 4.8% in the main quartzo-feldspathic minerals in schist/gneiss, (b) biotite 3.2%, and muscovite 9.6% amongst the micaceous minerals, (c) calcite 7.2% and pyrope garnet 0.5%, (d) 2.0% 4M pyrrhotite as the reactive iron sulfide, and (e) ferrihydrite 9.9% and ettringite 0.9% as the products of pyrrhotite oxidation, and resultant sulfate crystallization, respectively. Corresponding major element oxidation composition of concrete from XRF showed $SiO_2$ 50.86%, $Al_2O_3$ 11.03%, $Fe_2O_3$ 6.2%, CaO 13.45%, MgO 2.33%, $Na_2O$ 1.67%, $K_2O$ 1.61%, $TiO_2$ 0.52%, $SO_3$ 1.47%, LOI 10.67%.

For two MA foundations, XRD result of bulk concrete showed [7]: (a) quartz 39% (2002), 36.8% (2024), albite 21.6% (2002), 25.5% (2024), microcline 5.4% (2002), 3.6% (2024), orthoclase 5.6% (2024 in the main quartzo-feldspathic minerals in schist/gneiss, (b) biotite 0.4% (2002), 1.9% (2024), muscovite 17.6% (2002), 13.0% (2024), (c) illite 3.0% (2002), 0.9% (2024), kaolinite 1.5% (2002), chlorite 8.0% (2024) in clay minerals, (d) calcite 2.8% (2002), 2.8% (2024), (d) pyrrhotite 0.2% (2002) and 0.2% (2024) as the reactive iron sulfide, and (e) ettringite 8.5% (2002) and 1.7% (2024) from sulfate crystallization, ferrihydrite was below the detection limit. Corresponding major element oxidation composition of

concrete from XRF showed $SiO_2$ 53.3-58.6%, $Al_2O_3$ 12.8%, $Fe_2O_3$ 2.8-3.9%, CaO 9.9-10.6%, MgO 1.4-1.5%, $Na_2O$ 1-1.5%, $K_2O$ 2.7-3.2%, $TiO_2$ 0.48-0.52%, $SO_3$ 0.9-1.3%, LOI 8.5-11.5%.

## 4. CONCLUSIONS

In all three foundations, evidence of extensive pyrrhotite oxidation was clear from: (a) striated nature of oxidized pyrrhotite and associated reddish brown oxidation products while observing polished sections under a stereomicroscope, (b) spectacular parallel bands of Fe-O in pyrrhotite while observing a polished section in a reflected-light microscope or in SEM, (c) detection of ferrihydrite in XRD analysis in the CT foundation, and, (d) extensive cracking of pyrrhotite-bearing aggregates often extending into the paste. Evidence of subsequent ISA was more evident in the paste of crumbled Vernon, CT foundation where paste showed heavy infestation of fibrous ettringite not only as mere secondary precipitates in voids and/or cracks but more deleteriously within the porous to denser areas of paste often intimately mixed within the CSH where such formation of ettringite within the confined spaces in paste are the results of paste expansion and additional damage. SEM-EDS sulfate levels of paste in the present MA foundations (<1% S, atomic) are less than the paste sulfate in the present CT foundation, which, are still lower than sulfate levels found in other distressed foundations in CT [e.g., 1].

Contrary to extensive pyrrhotite distress of the much porous concrete blocks in the County Donegal in Ireland, where not only pyrrhotite oxidation but more profoundly ISA of sulfate-contaminated paste are found to be the primary mechanisms of crumbling of blocks, the dense concrete in the foundations of the eastern US homes along with some similar dense foundations in Ireland that the author has examined, it has appeared that perhaps the denser microstructure of concrete might have slowed down the distress by slowing the access of moisture and oxygen but as long as there is pyrrhotite and the availability of moisture and oxygen for its high reactivity, there is always the potential for distress, perhaps denser microstructure of concrete would facilitate oxidative expansion and perhaps additional distress from ettringite-related expansion in the confined spaces in paste as the more viable mechanisms than severe decomposition of paste *per se* from ISA as seen in the crumbled blocks in Ireland. In Canada, however, both the host rock of pyrrhotite (anorthositic gabbro) as well as the concrete foundation are pretty dense but still distress has reportedly occurred within 5 years of construction [3], indicating the complex nature of pyrrhotite deterioration in concrete.

To prevent future pyrrhotite-related distress, the United States Geological Survey has created a map of distribution of potentially pyrrhotite-bearing rocks [8]. Both CT and MA legislations are proposed for the much-needed steps to regulate testing of sand, gravel, and quarried stones. Along with our proposed performance-based testing protocol [4], our lab has been involved in testing of various quarries across CT and MA for pyrrhotite.

## 5. REFERENCES

[1] Jana, D., “Pyrrhotite Epidemic in Eastern Connecticut: Diagnosis and Prevention,” ACI Materials Journal V 117, No.1, January 2020, pp. 1-20.

[2] Jana, D., “Cracking of residential concrete foundations in eastern Connecticut, USA from oxidation of pyrrhotite,” Case Studies in Concrete Construction, Vol 16, 2022.

[3] Jana, D., “Concrete deterioration from the oxidation of pyrrhotite - A state-of-the-art review, Chapter 5, In “Pyrite and Pyrrhotite: Managing the Risks in Construction Materials and New Applications,” Michael L.J. Maher (editor), Nova Science Publishers, pp. 137-221.

[4] Jana, D., “Preventing pyrrhotite damage in concrete: Proposal for a performance-based testing protocol,” Concrete International, American Concrete Institute, 42(5), pp. 42-47.

[5] Substitute House Bill No. 6646, Connecticut Public Act No. 21-120: “An Act Concerning Crumbling Concrete Foundations,” State of Connecticut, July 6, 2021, 10 pp., www.cga.ct.gov/2021/act/Pa/ pdf/2021PA-00120-R00HB-06646-PA.PDF.

[6] Massachusetts Senate Bill No. 548, “An Act Relative to Crumbling Concrete Foundations,” The Commonwealth of Massachusetts, Feb. 18, 2021, 7 pp., https://malegislature.gov/Bills/192/S548.

[7] Jana, D., “From CT to MA: Case Studies of Crumbled Foundations from Pyrrhotite Oxidation and Internal Sulfate Attack in the Eastern US,” Data https://www.cmc-concrete.com/pyrrhotite-crumbling-foundations.

[8] Mauk, J.L.; Crafford, T.C.; Horton, J.D.; San Juan, C.A.; and Robinson, G.R. Jr., “Pyrrhotite Distribution in the Conterminous United States, 2020,” U.S. Geological Survey Fact Sheet 2020-3017, Mar. 2020, 4 pp.

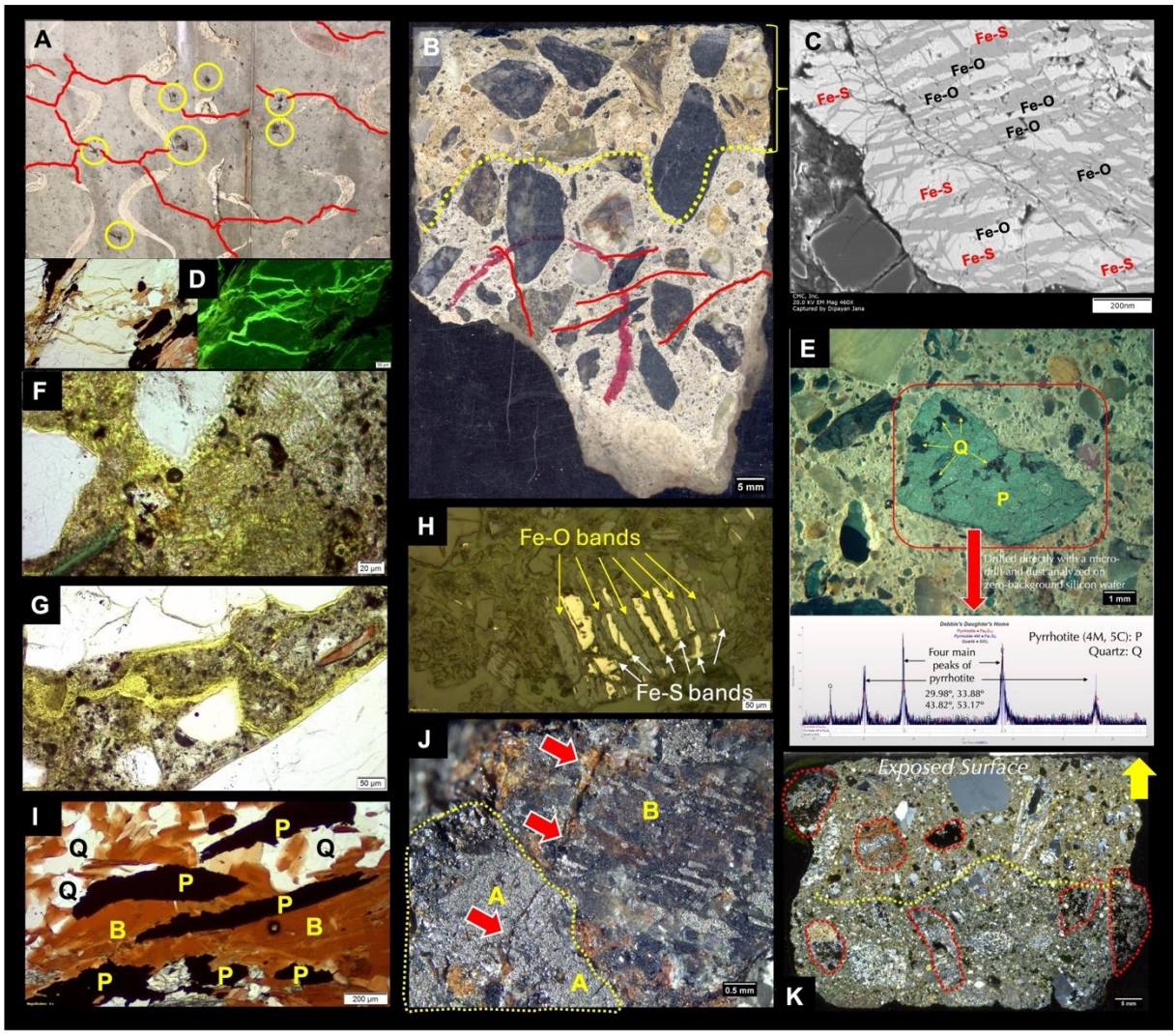


Figure 1: The Vernon, CT home. A: Extensive cracking (red lines) and popouts of oxidized pyrrhotite grains (circled) in the foundation wall. B: A polished concrete fragment showing beige discoloration at the exposed surface end of wall from atmospheric carbonation (depth of carbonation is 30-mm, which is marked by yellow dotted line as the carbonation front); visible cracks are marked with red lines. C: Backscatter electron image of a polished section of extensively cracked oxidized pyrrhotite grain showing alternate darker gray Fe-O and brighter Fe-S bands. D: Micrograph of thin section of an extensively cracked pyrrhotite-bearing coarse aggregate where cracks are highlighted by fluorescent dye in the corresponding image taken in the UV light. E: A sand-size 'chunk' of pyrrhotite with minor quartz inclusions, which has shown a spectacular four-peak diffraction pattern of 4M pyrrhotite. F: Micrograph of thin section showing extensive contamination and mixing of fibrous, acicular ettringite in cement paste, i.e., beyond the usual filling of voids and cracks by secondary ettringite, such ettringite-infested paste is the telltale evidence of ISA in paste. Ettringite-related ISA occurs only in the interior non-carbonated concrete since ettringite is unstable in the carbonated surface region of foundation, G: Cracks extending from unsound aggregates to interstitial paste, which are often filled with ettringite. H: Micrograph of polished section of oxidized pyrrhotite in the reflected-light mode of a petrographic microscope showing alternate Fe-O and Fe-S bands. I: Thin section micrograph showing close association of elongated pyrrhotite grains with biotite flakes in aggregate, where such juxtaposition pyrrhotite within biotite has fasciliated easy access of oxygen and moisture for oxidation through the biotite flakes. J: A pyrrhotite 'chunk' in a gneiss coarse aggregate showing one half of less oxidized (marked as 'A') and other half of extensively oxidized pyrrhotite, latter with parallel Fe-S bands (marked as 'B'), and a crack traversing the grain (red arrows) developed from oxidation. K: Large-area (50 × 75 mm) thin section scanned on a flatbed transparent scanner showing pyrrhotite-bearing aggregates (marked by red dotted lines) where thin section was sandwiched between two perpendicular polarizing filters to recreate cross-polarized light view of a petrographic microscope.

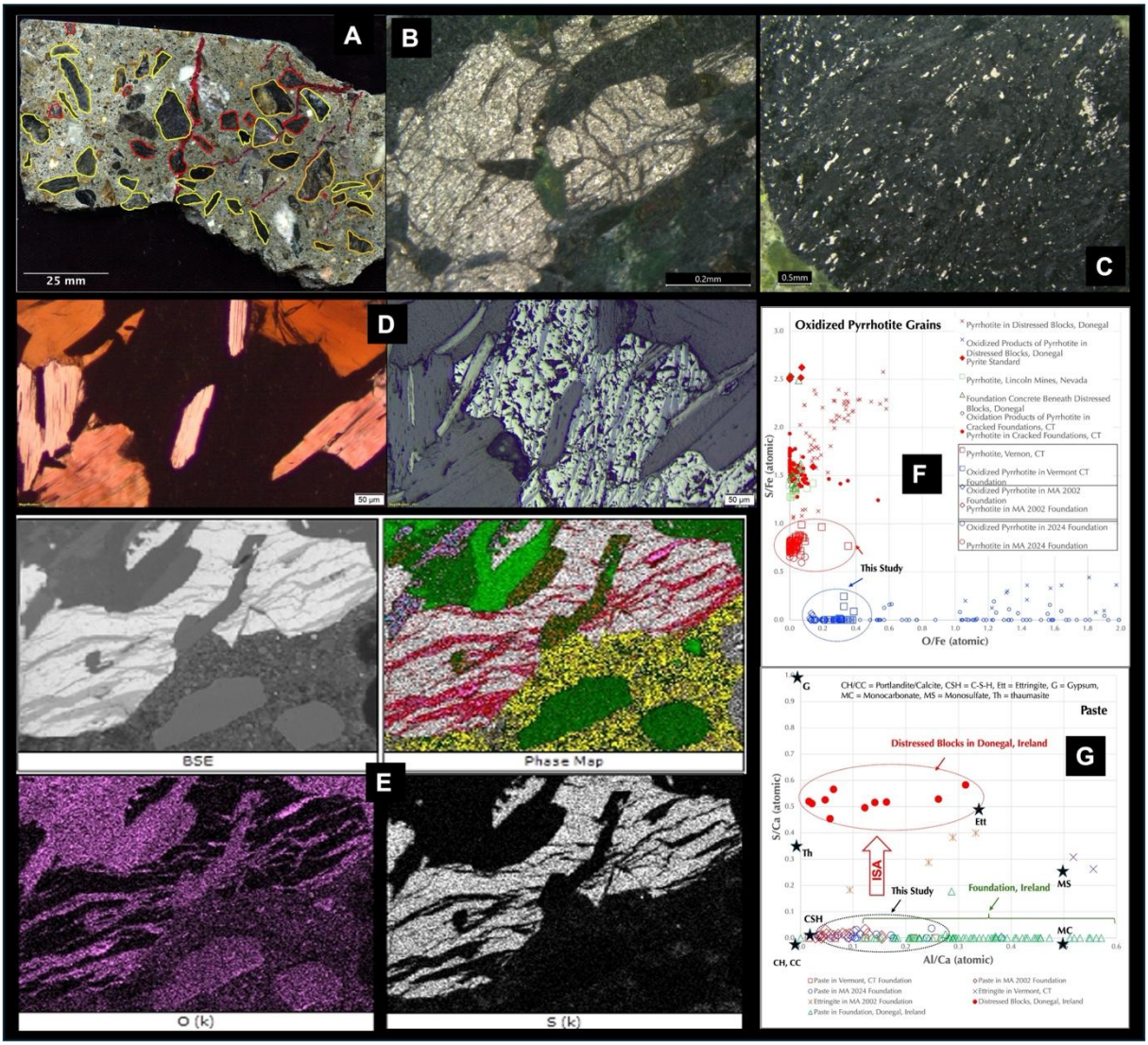


Figure 2: The Rutland, MA foundations. A: Polished cross section of a fragment where extensively and moderately pyrrhotite-bearing schist aggregates are marked by peripheral red and yellow lines, respectively, whereas non-pyrrhotite quartzite aggregates are marked in beige lines; a crack is marked in red line. B: Coarsely crystalline, subhedral to anhedral oxidized pyrrhotite grains showing characteristic striations. C: Finely disseminated forms of pyrrhotite either in random scattered grains or aligned along the weak planes of schistosity. D: Close association of pyrrhotite and biotite often one engulfed into another. E (four images): Backscatter electron image and phase map of an oxidized pyrrhotite from the elemental maps of oxygen (in pink) and sulfur (in white), omitting calcium for paste (in yellow) showing oxidized iron striations in iron sulfide matrix. F: SEM-EDS studies of iron oxide bands in oxidized pyrrhotite grains plotted in S/Fe vs. O/Fe atomic ratios from this study, other crumbled foundations from the eastern CT, and a few distressed concrete blocks and foundations from County Donegal, Ireland. G: SEM-EDS studies of paste showing the absence of elevated sulfate in the paste of dense concrete foundations from the eastern US or in some foundations in County Donegal, Ireland compared to the elevated sulfate levels ($S/Ca_{atomic}$ 0.4-0.6) from ISA in the distressed blocks of Ireland. Absence of elevated sulfate in the dense paste of foundations, however, does not necessrily indicate the absence of ISA when all available sulfate in the pore solutions are being used up in formation of ettringite in the confined spaces in paste to cause additional expansion and damage beyond the oxidative damage.